Light Metals 2012 *Edited by: Carlos E. Suarez*
TMS (The Minerals, Metals & Materials Society), 2012

SPECIFIC MOLECULAR FEATURES OF POTASSIUM-CONTAINING CRYOLITE MELTS

Galina Tsirlina[1], Evgeny Antipov[1], Dmitrii Glukhov[2], Alexander Gusev[3], Veronika Laurinavichute[1], Renat Nazmutdinov[2], Dmitry Simakov[3], Sergey Vassiliev[1], Tamara Zinkicheva[2]
[1] Laboratory for Basic Research in Aluminium Production, M.V.Lomonosov Moscow State University, Moscow, Russia
[2] Kazan National Research Technological University, Kazan, Republic Tatarstan, Russia
[3] Engineering and Technological Centre, Ltd., Krasnoyarsk, Russia

Keywords: Raman spectroscopy, Sodium and Potassium cryolite, Modelling of ionic species

Abstract

Experimental in situ Raman spectra are presented for potassium, sodium and mixed fluoroaluminate melts. More acidic melts with cryolite ratio (CR) below 2 are accented. The cation-dependent ratio of integral band intensities is assigned to specific interactions of potassium cations with low coordinated fluoroaluminates. For alumina containing melts, the effect of potassium on the stoichiometry of predominating oxofluoroaluminate anion is observed indirectly. Density functional theory is employed to investigate the behavior of different fluoroaluminates (including dimers) and their associates formed by alkali metal cations.

Introduction

The problem of inert anode [1] should be basically treated as a search of combination of anode material and melt composition favorable for as low degradation rate as possible. Low temperature acidic melts are sometimes assumed to be less risky because the solubility of any anode component tends to decrease, as compared to the melts of higher CR. However another important factor is the ionic melt composition: the decrease of Al coordination number at low CR can induce higher reactivity of metals and oxides [2].

Information concerning coordination numbers of fluoroaluminate melts is available from Raman spectroscopy data [3–6]. Quantum chemical approaches (see work [7] and Refs cited therein) are very helpful to gain important insight into the structure of cryolite melts, as well as to interpret experimental data [7–9]. Model Raman spectra have also been calculated in papers [10, 11] on the basis of classical molecular dynamics simulations. Our efforts are concentrated on combined experimental and computational studies of poorly investigated melts in a low CR interval. Earlier we extended this approach to the studies of individual $MF+AlF_3$ melts (M = Li, Na, K) [7–9], and highlighted the cation M effect on the behavior of ion pairs and the formation of fluoroaluminate dimers. In what follows we present new data related to ternary systems and demonstrate that formally estimated $CR = MF/AlF_3$ can deviate from real acidity CR_{true}. We define the latter as $CR_{true} = CN - 3$ (CN is the averaged coordination number); it depends on details of melt composition, not only on the alkaline metal/aluminum ratio.

Experimental

Spectroscopic measurements were performed using a fiber-optics Raman spectrometer RamanRXN1 (Kaiser Optical Systems) with a long-focal-length optics (working distance 430 mm). Laser wavelength was 532 nm. The scheme of experimental setup and experimental details are available in Refs [7, 8].

For melt preparation, thoroughly purified reagents (MF, AlF_3 and Al_2O_3) were used, M = Na or K. The reagent mixture (typically 10 g) was melted in a platinum crucible. Low temperature melts of CR 1.3 was studied. The liquidus temperature of $NaF-KF-AlF_3$ melts was estimated using the data in Ref. [12].

For a quantitative analysis of the spectra, we used deconvolution of the experimental bands (Gaussian-Lorenzian fit, Thermo Grams/AI 8.0 software). To reduce the uncertainty, usually we assumed fixed Lorentzian contributions for bands in one series of Raman spectra. Band assignment to certain species is based on simplified consideration of monomeric fluoroaluminates [7].

Details of quantum-chemical calculations

The quantum chemical calculations were performed at the DFT level by using the B3LYP hybrid functional as implemented in the Gaussian 03 program package [13]. Our calculations are related to neutral ensembles, with the charge excess of anionic Al(III) complexes compensated by the cations. We thus assume that the formed ion pairs (small clusters) address the short – range effects of the ionic environment. For the description of Al, F, Na and K atoms the standard triple-zeta 6–311G valence basis set augmented by polarization (d) functions was employed. The geometries of the Al(III) complexes were fully optimised in the gas phase without symmetry constrains. We used the program ChemCraft [14] for the visualization of model Raman spectra; the calculated frequencies were not scaled.

Results and discussion

Ternary $MF+AlF_3$ systems.

Evolution of Raman spectra with increase of Na+ mole fraction in acidic NaF+KF+AlF3 melts is demonstrated in Fig.1. The most strong bands at ca. 620 and ca. 555 cm-1 can be assigned to four- and five-coordinated aluminum in fluoride complexes, respectively. The main discovered tendencies for these bands are as follows:

— band frequency increases for both AlF_4^- (5 cm^{-1}) and AlF_5^{2-} (10 cm^{-1}), Fig. 2a;
— fraction of AlF_4^- decreases with increase of Na^+ fraction, when the fraction of AlF_5^{2-} increases;
— bands half-width increases with Na^+ content, the effect being stronger for AlF_5^{2-}, Fig. 2b.

To understand a possible molecular reason of these effects, we considered the formation of ionic associates of fluoroaluminate species with K^+, Na^+ and both these cations simultaneously.

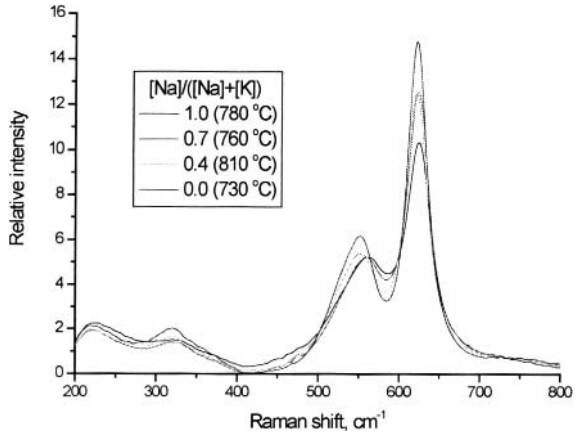

Fig.1. Series of experimental Raman spectra obtained for the melts at formal CR 1.3 and various Na^+ content. All the spectra are normalized per total area of overlapping peaks.

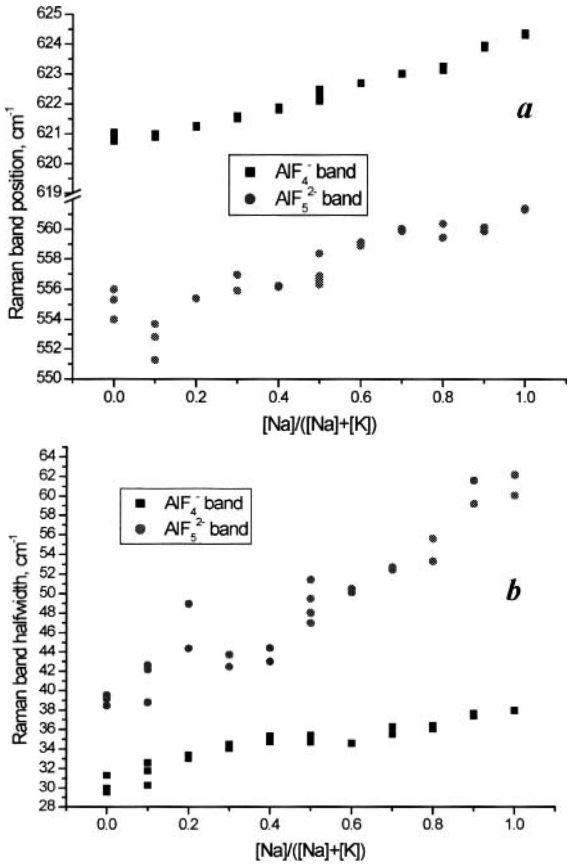

Fig.2. Effect of Na^+ mole fraction on the AlF_4^- and AlF_5^{2-} band frequency (a) and halfwidth (b) for the melts of formal CR 1.3. The position of AlF_4^- band was extrapolated to the fixed temperature (760 °C). Correction was carried out be means of interpolation, with the use of experimental temperature dependence of this band position in $NaF+AlF_3$ melt. In 730–820 °C interval the temperature dependence is very close to linear, and the difference of band frequencies at the edges is ca. 2 cm^{-1}.

Two local energy minima were found for $AlF_4^-•K^+$, where the cation K is projected either to the face of tetrahedral Al(III) complex (*i*), or to its ridge (*ii*). The geometrical structures are shown in Fig. 3. The same conformations were found previously for an $AlF_4^-•Na^+$ pair [7]. The position of main peaks of the model Raman spectra for the most stable structure (*i*), 619 cm^{-1}, reveals a very slight red shift as compared with that for $AlF_4^-•Na^+$, 620 cm^{-1} [7], which at least does not contradict experiment. Previously we investigated $AlF_5^{2-}·2K^+$ associate and found only one stable conformation (*i*) (see details in Ref. 9), while for $AlF_5^{2-}•2Na^+$ two structures exist [7]. In the present work three different stable structures were found for a mixed associate $AlF_5^{2-}•Na^+•K^+$ which are shown in Fig.4, *(i) – (iii)*. Conformation *(i)* has the deepest energy. A mixed dimeric associate $Al_2F_{11}^{5-}•5X^+$ (X^+ = Na and K) was modeled as well in order to address the effect of bridged fluoroaluminate complexes (see *(iv)* in Fig. 4). Such a dimer can be observed in the large clusters modeling fragments of molten cryolite at low CR [9]; its stoichiometry is close to that suggested earlier in Ref. 7 ($Al_2F_{10}^{4-}•4Na^+$).

As can be seen in Table 1, increasing the number of Na^+ ions in the model associates leads to the band frequency increase for both AlF_5^{2-} (6 cm^{-1}) and $Al_2F_{11}^{5-}$ (19 cm^{-1}) complex forms, in qualitative agreement with experiment.

Table 1. Calculated Raman frequencies (cm^{-1}) for symmetric stretching frequencies of neutral ionic pairs $AlF_5^{2-}·2X^+$ (X^+ = Na^+ or K^+, structure *(i)* in Fig.4) and for the main band for dimer species associated with cations, various Na^+/K^+ ratios.

Neutral ion pairs		Neutral associates of the dimers	
Species	Frequency	Species	Frequency
$AlF_5^{2-}•2K^+$	550	$Al_2F_{11}^{5-}•5K^+$	468
		$Al_2F_{11}^{5-}•4K^+•Na^+$	467
$AlF_5^{2-}•K^+•Na^+$	552	$Al_2F_{11}^{5-}•3K^+•2Na^+$	470
		$Al_2F_{11}^{5-}•2K^+•3Na^+$	475
$AlF_5^{2-}•2Na^+$	556	$Al_2F_{11}^{5-}•K^+•4Na^+$	476
		$Al_2F_{11}^{5-}•5Na^+$	487

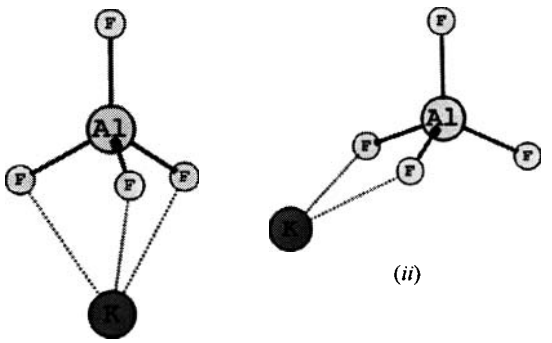

Fig.3. Optimized geometry of two different structures obtained for a model associate $AlF_5^-•K^+$.

The most important geometric effect of the alkali cation nature discussed in Ref. 9 is the cation location in ionic associates. When going from Li^+ to Na^+ and then to K^+, typical location is changed in the following sequence: vertex, edge, and then facet. The same

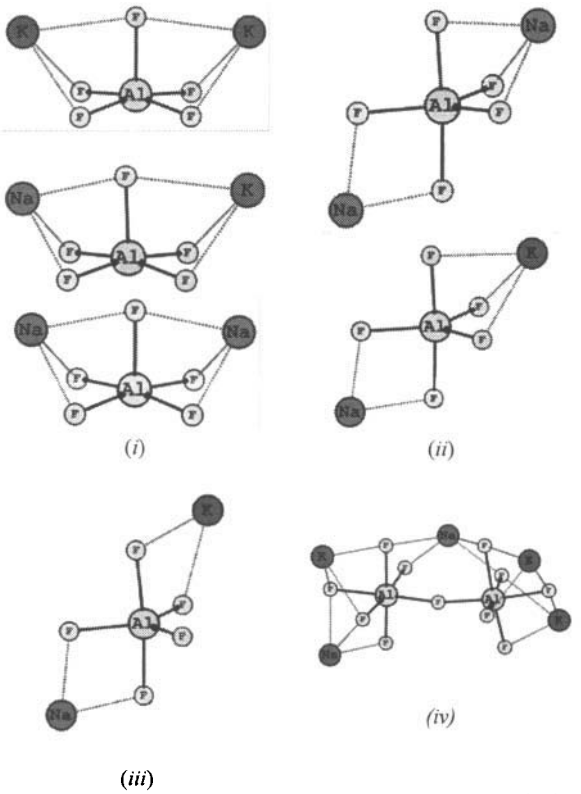

Fig.4. Optimized geometry of three different structures obtained for a mixed associate $AlF_5^{2-}•Na^+•K^+$, and example of the optimized structure of dimeric associate $Al_2F_{11}^{5-}•5X^+$ ($X^+ = 2Na^+$ and $3K^+$). The structures of *(i)* and *(ii)* associates with $2Na^+$ and $2K^+$ exclusively are shown for comparison.

trend can be observed for crystal lattices of various solid fluorometalates [15]. As one can conclude from Fig. 4, these trends are the same for mixed associates, i.e. monotonous changes of any vibrational features are expected for the series of $NaF+KF+AlF_3$ melts.

The effect of cations on the structure of fluoroaluminate ionic associates results in pronounced difference of thermodynamic properties for binary systems of various cationic composition [9]. Now we can expect that the same is true for the ternary systems with two sorts of cations as well. In particular, CR_{true} value (presenting the averaged coordination number of Al) is expected to vary smoothly with cations ratio.

Ternary $MF+AlF_3+Al_2O_3$ systems.

Raman behavior of $KF+AlF_3$ and $NaF+AlF_3$ melts of CR 1.3 after addition of various quantities of alumina is shown in Figs 5a and 5b respectively. For the former system, the effect is more visible. The effect on band intensity is mostly observed for AlF_4^- band, when AlF_5^{2-} undergoes more pronounced broadening. Rough semi-quantitative analysis demonstrates the increase of Al–F coordination number resulting from interactions of fluoroaluminates with alumina.

To consider possible equilibria more quantitatively, we treated the data for integral intensity of the stronger AlF_4^- band (solid line in Fig.6). The dependence of this quantity on alumina content in the melt was compared with calculated dependences expected for various stoichiometry of oxofluoroaluminates, assuming the following possible equilibria

$$Al_2O_3 + 4AlF_3 + 3xF^- = 3Al_2OF_{4+x}^{x-} \quad (1)$$

or

$$2Al_2O_3 + 2AlF_3 + 3xF^- = 3Al_2O_2F_{2+x}^{x-}, \quad (2)$$

and also various x coefficients. The best agreement with experiment was found for reaction

$$Al_2O_3 + 5AlF_4^- = 3\,Al_2OF_5^- + AlF_5^{2-}, \quad (3)$$

which corresponds to formation of four-coordinated Al in the dimers with two bridging ligands (O and F). Simultaneous formation of five-coordinated species explains the observed redistribution of Raman bands.

Our results demonstrate that CR_{true} of alumina-containing potassium melt is higher than the formal CR calculated as the ratio of initially mixed potassium and aluminum fluorides.

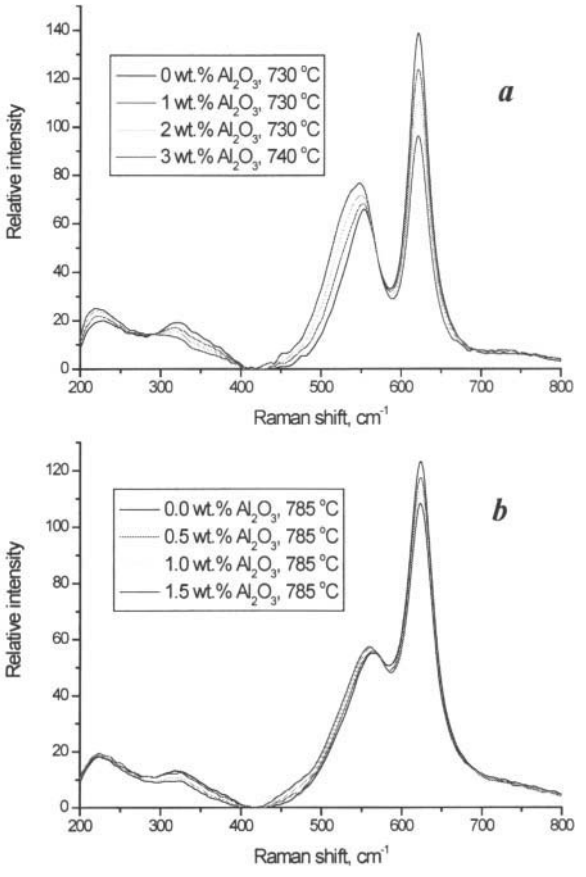

Fig.5. Series of experimental Raman spectra obtained for potassium (a) and sodium (b) melts of formal CR 1.3 and various alumina content. All spectra are normalized per total area of overlapping peaks.

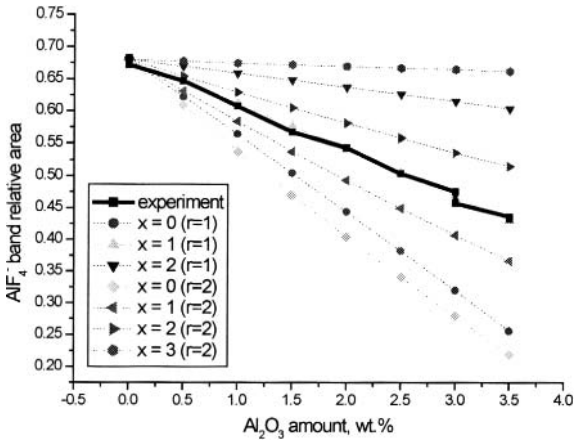

Fig.6. Relative AlF_4^- Raman band area concentaration dependence measured experimentally (solid line) and calculated for different stoichiometry and Raman activity of oxofluoroaluminate complexes. KF-AlF_3 melt of formal CR 1.3. Single or double Raman activity of dimer oxofluoroaluminate as compared with monomer fluoroaluminates is noted by parameter *r*.

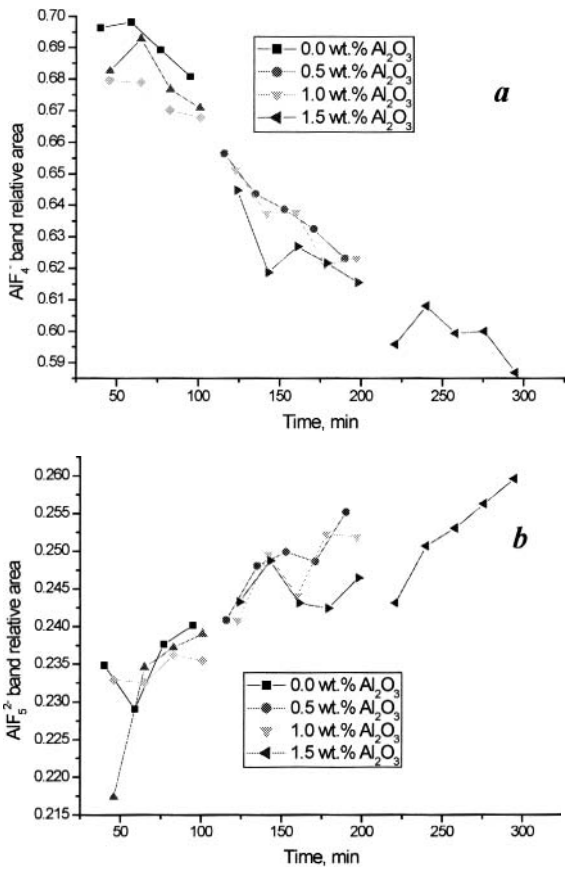

Fig.7. Time dependence of relative AlF_4^- (a) and AlF_5^{2-} (b) Raman band area at different Al_2O_3 concentration in sodium melt of formal CR 1.3.

Similar data treatment for sodium-based system (Fig. 5b) was less successful, as demonstrated contradictory results. We assume that the problem goes from much faster evaporation of this melt, with predominating loss of 4-coordinated species in the form of $NaAlF_4$ (note that the temperature is much higher for sodium melt as compared to potassium melt of the same formal CR). This hypothesis is confirmed by time dependence of intensities (Fig.7).

Approximate treatment demonstrates that the value of x for sodium melt is higher as compared to potassium melt. The most realistic assumptions for sodium melt is the reaction

$$Al_2O_3 + 2AlF_4^- + 2AlF_5^{2-} = 3Al_2OF_6^{2-}. \quad (4)$$

However we can not also exclude some processes associated with reaction (2). In any case, for sodium melt the equilibria with alumina are expected to result in lower CR_{true}, but this effect is more or less compensated by selective melt evaporation.

Conclusions

Complex equilibria in the ternary (K, Na)F+AlF_3 and MF+AlF_3 + Al_2O_3 systems result in formation of species, which structure depends on the nature of cation. Principle difference in location of sodium and potassium cations in ion pairs formed with fluoroaluminate anions is predicted at computational level, and reasonability of computational modeling is confirmed by spectroscopic means. The difference in macroscopic (thermodynamic) properties of sodium, potassium and mixed melts can be solidly explained by the difference in anion-cation interactions. The most important is the effect of cation nature on stability of various fluoro- and oxofluoroaluminates, which results in higher CR_{true} in potassium melts of the same stoichiometry, and in the difference of molecular composition of oxegen-containing species predominating in sodium- and potassium-based melts.

Acknowledgements

This study was performed in the framework of "RUS Engineering" – MSU agreement.

References

1. *Inert Anodes for Aluminium Elecrolysis*, 1st edition, I.Galasiu, R.Galasiu, J.Thonstad, Aluminium-Verlag, Germany, 2007
2. S.Yu.Vassiliev, et al., *Microstructural aspects of the degradation behavior of SnO_2-based anodes for aluminum electrolysis*, J. Electrochem. Soc., 157 92010) C178-C18.
3. B. Gilbert, S.D. Wiliams, G. Mamantov, *Raman Spectroscopy of Fluoride-Containing Chloroaluminate Melts*, Inorg. Chem. 27 (1988) 2359-2363.
4. F. Auguste, et al., *The Dissociation of Fluoroaluminates in FLiNaK and CsF-KF Molten Mixtures: A Raman Spectroscopic and Solubility Study*, Inorg. Chem. 42 (2003) 6338-6344.
5. E. Tixhon, E. Robert, B. Gilbert, *The molten MF-AlF_3-MCl system (M= K, Na): A study by Raman spectroscopy*, Vibr. Spectrosc. 13 (1996) 91-98.

6. B. Gilbert, et al., *Structure and Thermodynamics of NaF-AlF_3 Melts with Addition of CaF_2 and MgF_2*, Inorg. Chem. 35 (1996) 4198-4210.

7. R. R. Nazmutdinov, et al., *A spectroscopic and computational study of Al(III) complexes in sodium cryolite melts: Ionic composition in a wide range of cryolite ratios*, Spectrochim. Acta A, 75 (2010) 1244-1252.

8. S. Vassiliev, et al., *In situ Raman experimental study of ionic species in cryolite melt of various composition*, Light Metals (2010) 559-561.

9. R. R. Nazmutdinov, et al., *A Spectroscopic and Computational Study of Al(III) Complexes in Cryolite Melts: Effect of Cation Nature,* Spectrochim. Acta A, submitted.

10. Z. Akdeniz, P.A. Madden, *Raman spectra of ionic liquids: a simulation study of AlF_3 and its mixtures with NaF*, J. Phys. Chem. B, 110 (2006) 6683-6691.

11. S. Usar, S. Cikit, Z. Akdeniz, *A simulation study and theoretical Raman spectra of cryolitic melts*, J. Optoelectronics and Advanced Materials 11 (2009) 1384-1387.

12. A.Apisarov, et al., *Liquidus temperatures of cryolite melts with low cryolite ratio*, Light Metals (2010) 395-398.

13. Gaussian 03, Revision B.04, M. J. Frisch, et al., Gaussian, Inc., Pittsburgh PA, 2003.

14. http://www.chemcraftprog.com .

15.Inorganic Crystal Structure Database (ICSD), Fachinformationszentrum Karlsruhe (FIZ) and National Institute of Standards and Technology (NIST), Version Release 2008/1.